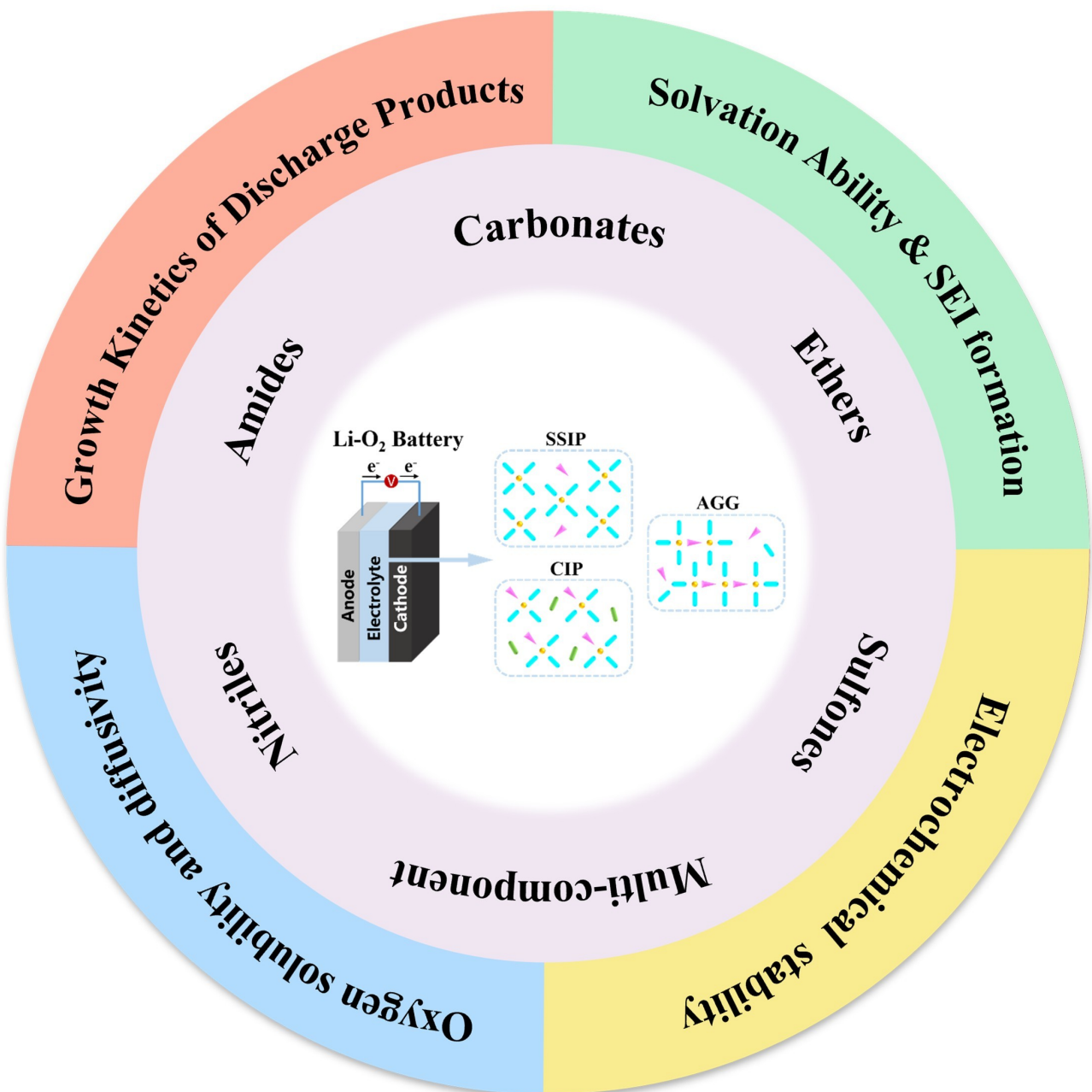


Non-Aqueous Liquid Electrolytes for Li-O₂ Batteries

Shu Wang,^[a] Haohan Yu,^[a] Zerui Fu,^[a] Dapeng Liu,^{*[a]} and Yu Zhang^{*[a, b]}



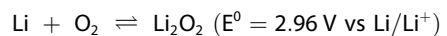
Li-O₂ batteries (LOBs) have become a research hotspot of energy storage devices because of its high theoretical energy density. Practical applications require that non-aqueous LOBs can deliver stable and high reversible capacity, which heavily depends on the appropriate electrolyte system. Therefore, it is very important to select electrolytes that are hard to decompose and conducive to modulating the growth kinetics of

discharge products. Herein, we will review the current progress and challenges of non-aqueous liquid electrolytes for LOBs by analyzing the influence factors on electrolyte stability and introducing the design and modification methods of electrolytes with different solvent types. At last, the possible research tactics have been proposed to develop advanced electrolytes for improving electrochemical performance of LOBs.

1. Introduction

Aiming at efficient energy utilization, the imperative lies in developing advanced energy storage technologies. As one of the most promising candidates, Li-O₂ batteries (LOBs) have drawn intensive attention due to exceptional theoretical energy density (~3500 Wh kg⁻¹), which have been considered as frontrunners for the next-generation electric vehicles. Excitedly, recent research shows that the cycle life of LOBs has been improved to be as high as 1000 times, closely meeting the growing demands of consumers.^[1]

The first non-aqueous LOB was reported by Abraham and coworkers in 1996, the total reaction of which could be described as follows:^[2]



During the discharge process, Li metal is oxidized to Li⁺ that will be fast solvated into electrolytes, and then migrate from anode to cathode, and finally react with the reduced O₂ to produce Li₂O₂ at cathode. While for charge, Li₂O₂ is reversibly decomposed into Li⁺ and O₂, and Li⁺ migrates from cathode to anode by aid of electrolytes and finally reduced into Li metal at anode.^[3] Obviously, electrolytes are in charge of Li⁺ transport between electrodes, and meanwhile interact with electrodes to form metastable interfaces. Especially for non-aqueous liquid electrolytes, they have contributed significantly to improving the energy density of LOBs compared with those aqueous ones.^[4] At present, studies on electrolytes are primarily focused on their electrochemical stability, solvation ability, capacity for Li⁺ transport, influence on the growth kinetics of discharge products, and construction of solid electrolyte interface (SEI) on anode.^[5]

As the linker of cathode and anode, electrolyte usually plays complex roles in determining battery performance. Firstly, the formation of SEIs should be dependent on the solvation structure of Li⁺, arising from intricate coordination interactions among solvent, anion, and Li⁺. Huang et al.^[6] proposed the concept of strong solvated electrolytes (SSE) and weak solvated

electrolytes (WSE). In SSE, Li⁺ is isolated from anions by interacting with solvent to form a solvent-separated ion pairs (SSIPs). After coordinated with Li⁺, the lowest unoccupied molecular orbital (LUMO) energy of solvent molecules decreases, making them easier to be reduced by Li metal.^[7] This process induces the formation of organic-rich SEIs with low Li⁺ conductivity and mechanical strength that fails suppressing the growth of Li dendrites. As a result, reversibility and coulombic efficiency (CE) are seriously limited. The anions in WSE solvated shells with lower solvation capacity than SSE can replace partial solvent molecules to participate in the solvated sheath of Li⁺ so as to form two types of ion pairs (contact ion pairs (CIPs) and aggregated ion pairs (AGG)), generating the inorganic-rich SEIs. The concentrated inorganic components favor enhancing mechanical strength, accelerating Li⁺ transfer, and inducing uniform Li deposition.^[6]

Secondly, the solubility of the dissolved LiO₂(sol) and/or O₂⁻(sol) in electrolyte strongly affects the growth of Li₂O₂ to abide by either the solution or the surface rules. In the high donor number (DN) electrolytes, LiO₂(sol) is apt to disproportionate into Li₂O₂ that would further grow into large sized toroids according to the solvation-mediated pathway. While in the low DN electrolytes, the surface-adsorption pathway becomes dominant that Li₂O₂ tends to grow into compact film-like structures on cathode. As a result, the former often contributes to a higher battery capacity as well as a lower overpotential if compared to the latter.^[8] According to the frontier molecular orbital theory, if the LUMO energy of electrolyte is low, it is prone to decompose into SEI at anode, and meanwhile if the highest occupied molecular orbital (HOMO) energy is high, it will be oxidized at cathode. Those highly sensitive intermediate free radicals and singlet oxygen will attack electrolyte during charge/discharge, resulting in its decomposition and eventually battery failure.^[9]

This paper provides a brief overview on the resent research progress and challenges on electrolytes for LOBs with different solvents containing lithium salts and additives. Non-aqueous electrolytes exhibit excellent Li⁺ transport capabilities and completely contact with anode materials, which could be classified into carbonates, ethers, nitriles, sulfones, and amides according to the types of substances. The discussions revolve around the design and modification of electrolytes using various kinds of solvents along with special additives and redox mediators. At last, the prospects for the development of electrolytes are presented, hoping that the review can be of assistance to those engaged in LOBs.

[a] S. Wang, H. Yu, Z. Fu, D. Liu, Y. Zhang

Key Laboratory of Bio-inspired Smart Interfacial Science and Technology of Ministry of Education, School of Chemistry, Beihang University, Xueyuan Road 37, Beijing 100191, P. R. China
 E-mail: liupd@buaa.edu.cn
 jade@buaa.edu.cn

[b] Y. Zhang

Beijing Advanced Innovation Center for Biomedical Engineering, Beihang University, Xueyuan Road 37, Beijing 100191, P. R. China

2. Non-Aqueous Liquid Electrolyte

Currently, rational screening of solvents remains a significant challenge in electrolyte development. Several solvent descriptors including DN, polarity, electrostatic potential (ESP), and some other pertinent indicators have been successfully employed to evaluate the Li^+ solvation structure.^[10] Among them, DN could be used to describe the ability of solvent to separate salt into ions, polarity could give expression to the inhomogeneity of the charge distribution in the solvent molecules, and ESP can simply and directly reflect the unbalanced distribution of charge between Li^+ and solvent.

2.1. Carbonate Electrolytes

Carbonate electrolytes have been widely employed in Li-ion batteries (LIBs), which are commonly characterized by low DN value and volatility. Linear carbonates are of low polarity, while cyclic ones are of moderate polarity.^[11] In 2005, Bruce et al.^[12] achieved a passable battery performance up to 50 cycles by using propylene carbonate (PC) as LOB electrolyte. Although thus as-obtained LOBs could operate in this way, however, further investigation revealed that carbonates would react with Li anode and be susceptible due to attack from discharge intermediates.

At anode, the LUMO energy level of the carbonate electrolyte is low, resulting in poor stability towards lithium metal. It triggers side reactions to form fragile organic-rich SEIs and thus induces uncontrollable Li dendrite growth.^[7] To address this issue, a solvation structure dominated by the high-DN anion of NO_3^- can be used to produce a stable Li_2O -rich SEI. However, LiNO_3 is difficult to be dissolved in carbonate electrolytes, so it needs to introduce a cosolvent such as ethylene glycol diacetate (EGD) to improve the solubility of LiNO_3 . The carbonyl groups of EGD will repel NO_3^- by electrostatic forces, thus

inhibiting the recombination of Li^+ and NO_3^- . As a result, it not only increases the solubility of LiNO_3 , but also reduces the solvent content in the inner layer of solvation structures. The promoted desolvation of Li^+ facilitated the formation of more NO_3^- derived SEIs at anode.^[7] Fluorination of carbonates is another emerging method to enhance the stability of Li anode. Highly fluorinated electrolytes are appealing to directly improve the evolution of Li^+ solvation sheath. Fast Li^+ desolvation induced the formation of stable LiF-rich SEIs accompanied by inhibition of Li dendrites, arousing high-quality SEIs for more stable battery cycling.^[13]

Besides poor stability of Li anode, decomposition of carbonates themselves is also a big problem. Zhang et al. studied the main gas components released during charge.^[14] For the first cycle, O_2 could be identified as the primary gas component, whereas CO_2 began to be predominant during the recharge processes. The following investigations reveal that ethylene carbonate (EC) possesses a high density functional theory (DFT) barrier,^[15] and after ab initio calculations, it has been shown that the ethylene group in EC is the key reactive moiety allowing the attack of ${}^1\text{O}_2$. The initial step of EC decomposition is the combination of two H atoms with singlet oxygen (${}^1\text{O}_2$), forming H_2O_2 and vinylene carbonate (VC).^[16] In another case, Bruce and coworkers^[17] proposed the possible reaction process as depicted in Figure 1a that O_2^- would undergo nucleophilic attack on CH_2 group via the bimolecular nucleophilic substitution ($S_{\text{N}}2$) mechanism, resulting in the ring-opening decomposition of PC. The Fourier transform infrared spectra (FTIR) in Figure 1b present the significant signal of Li_2CO_3 in the discharge products. Due to electrolyte decomposition, byproducts continued to accumulate at cathode during cycling, leading to the rapid degradation of LOBs. Based on the above studies, it could be found that carbonate electrolytes would decompose to different degrees during the charge/discharge cycles, and the poor chemical stability seriously limits their applications for LOBs.



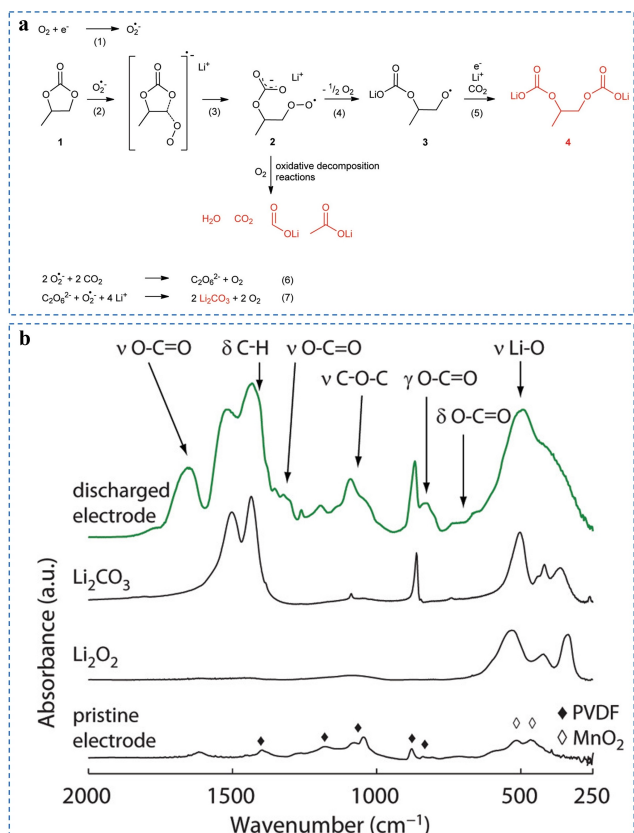
Yu Zhang received his Ph.D. degree from Jilin University in 2007. Then, he worked as a New Energy and Industrial Technology Development Organization fellow at Hiroshima University, Japan. He joined Beihang University in 2013 and now is a full professor of the School of Chemistry. He has worked for over 11 years in advanced energy materials, especially for optimizing electrode structures in the Li-air and Li/Na-ion battery field.



Biographical Sketch. Shu Wang is currently a graduate student at the School of Chemistry, Beihang University. Her current research interests primarily focus on optimization and design of electrolytes for $\text{Li}-\text{O}_2$ batteries.



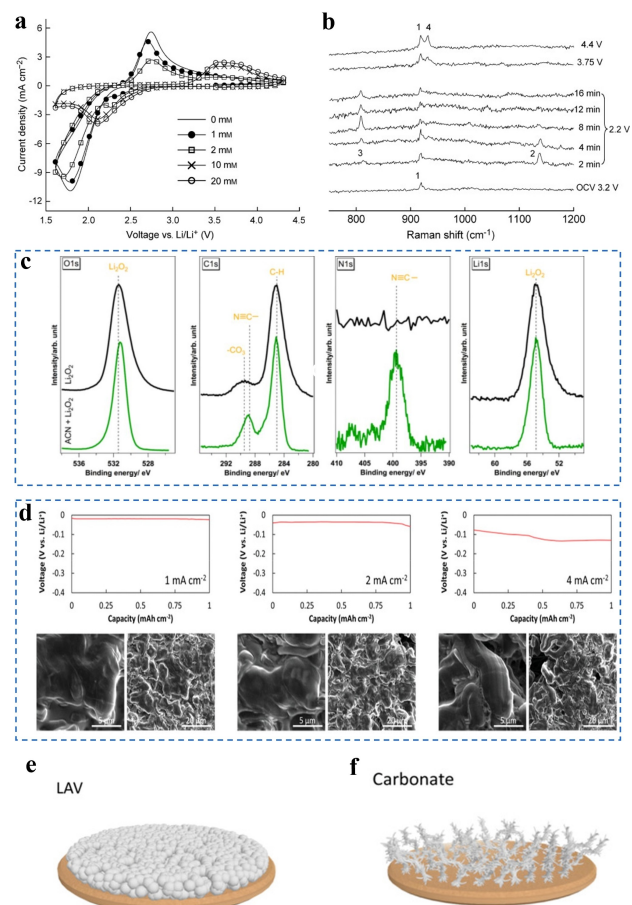
Dapeng Liu received his Ph.D. degree from Jilin University in 2008. During 2008–2012, he finished his postdoctoral research and worked as an associate professor at Changchun Institute of Applied Chemistry, Chinese Academy of Sciences. Then, he joined the School of Chemistry, Beihang University in 2013. His research mainly focuses on inorganic energy and catalytic materials.



2.2. Nitrile Electrolytes

Nitriles are also a type of low DN electrolyte, whose lowest negative and maximum positive ESP values are relatively high.^[18] Compared to others, acetonitrile (AN) electrolytes could exhibit excellent stability towards O₂⁻ and Li₂O₂ as evidenced by the data in Figure 2a and 2b.^[19] Vegge et al. analyzed the surface of the Li₂O₂ powder in direct contact with the nitro groups at different exposure times by using X-ray photoelectron spectroscopy (XPS) and no electrolyte decomposition was found (Figure 2c).^[20] Although AN is stable with superoxide and Li₂O₂, it is thermodynamically unstable in the presence of Li metal. Therefore, Li anodes need to be protected by forming a dense SEI layer with additives or by preparing an artificial passivation layer.

High-concentration AN electrolytes with addition of VC have been proven to be effective to suppress Li⁺ depletion at high current densities,^[21] and the optimal Li bis(fluorosulfonyl)imide (LiFSI)-AN-VC (LAV) electrolyte was determined to be [LiFSI]:[AN]:[VC] = 0.52:1.00:0.09. In Figure 2d and e, the Li deposition conducted at 1 mA cm⁻² in the LAV electrolyte typically exhibited a compact nodule-like structure with round-shaped edges. Moreover, this configuration can be maintained at the higher current densities of 2 and 4 mA cm⁻².



The typical dimension of the nodule-like Li particles is in the order of 10 μm, and they are very densely aggregated. Compared to mossy Li deposits (Figure 2f), this structure not only inhibits dendrite growth but also reduces the contact area between the deposited Li and electrolyte. In addition, an appropriate Li salt can also affect the composition of SEIs. LiNO₃ might be dual-use as an electrolyte salt and the SEI stabilizer.^[22] The reduction of LiNO₃ on Li metal would lead to the formation of Li₂O in favor of obtaining the inorganic-rich SEIs. Another soluble product, LiNO₂, could exhibit electroactivity within the operating potential window of LOBs and regenerate LiNO₃.

Rochefort et al.^[23] immersed Li metal in vinyl fluoride carbonate (FEC) to generate an electrochemically stable artificial

passivation layer at the Li metal/electrolyte interface through spontaneous decomposition of solvent, which prevents acetonitrile (ACN) reduction and thus allows the use of AN-based electrolytes in batteries. Compared to the layer derived from the decomposition of EC/diethyl carbonate (DEC), this artificial passivation layer extends the battery's cycle life. Besides AN electrolytes, Cui et al.^[24] reported a successful example of succinonitrile (SN)-based dual-anion deep eutectic solution (D-DES). In this D-DES, salt anions act as film-forming agents, modifying the Li interface and facilitating rapid Li^+ ion flux and uniform Li nucleation. As a result, this D-DES exhibits good ionic conductivity and enhanced electrode/electrolyte interface stability, leading to excellent lithium plating/stripping performance.

2.3. Ether Electrolytes

As a typical class of solvents with intermediate DN, ether-based electrolytes have been extensively investigated for applications in LOBs. The oxidation potential of ethers often exceeds 4.5 V (vs Li/Li⁺), and the wide electrochemical window adapted to the operating potential of LOBs endows them good stability. In the case of those with higher molecular weights, such as tetraglyme (TEGDME), they are of low volatility and high dielectric constant. Compared to carbonates, ether-based electrolytes feature lower viscosity and better O₂ transport ability, enhancing the ability of electrolyte to dissolve lithium salts. Additionally, ethers could demonstrate higher stability than carbonates towards O₂ species.^[25] McCloskey and co-workers^[26] found that the battery using a P50 cathode and 1 M LiTFSI in dimethoxyethane (DME) as electrolyte had the closest consumption to 2e⁻/O₂ during discharge and gave the best Li₂O₂ yield (91%).

In spite of this, ether-based electrolytes still have decomposition problems in the presence of oxygen and during prolonged discharge. Chen et al.^[27] found that the ether-based electrolytes underwent auto-oxidation after 8 d if exposed to pure oxygen, and the hydroxyl stretch band was significantly enhanced, while the characteristic signals of ethers were weakened in certain degrees (Figure 3a). Moreover, solvent auto-oxidation increased the decomposition of electrolytes during discharge. At the same time, the discharge capacity and operating potential have been more or less decreased (Figure 3b and c). Therefore, whether the battery is working or not, the ether solvent is oxidized when it comes into contact with oxygen. Reactive oxygen species such as O₂⁻ produced by cathode would also attack the electrolyte, leading to oxidative decomposition during long-term cycling. Thus, it is very important to understand the decomposition mechanism of ether electrolytes. Zhao et al.^[28] have been focused on the decomposition mechanism of TEGDME in the presence of oxygen as shown in Figure 3d. They found that O₂⁻ attacked the hydrogen atom in TEGDME with high chemical shift and generated a large amount of H₂O molecules. H₂O could react with the discharge product of Li₂O₂ at cathode to form LiOH and meanwhile migrate to Li anode and generate H₂, resulting

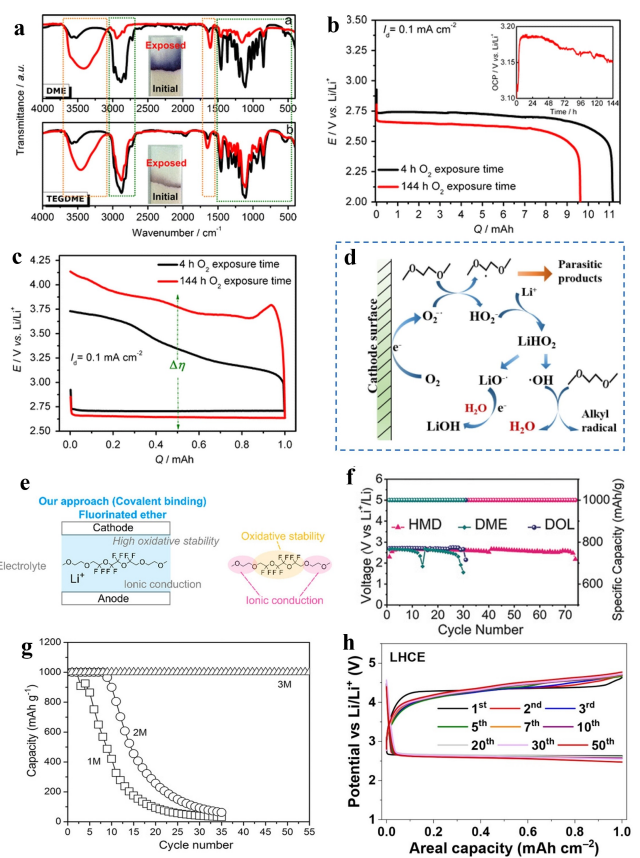


Figure 3. a) FTIR spectra of DME and TEGDME before and after prolonged oxygen exposure. Reproduced with permission from Ref.^[27] Copyright (2013) Springer-Verlag Berlin Heidelberg. b) Discharge curves of the DME/DOL-based cell which operated after being exposed to oxygen for 4 h and 6 days. Reproduced with permission from Ref.^[27] Copyright (2013) Springer-Verlag Berlin Heidelberg. c) Discharge-charge profiles of the DME/DOL-based cell which operated after being exposed to oxygen for 4 h and 6 days. Reproduced with permission from Ref.^[27] Copyright (2013) Springer-Verlag Berlin Heidelberg. d) The proposed reaction steps at the cathode on discharging a LOBs. Reproduced with permission from Ref.^[28] Copyright (2021) ELSEVIER B.V. and Science Press. e) Covalently attaching an ether to the hydroperfluoroether allows for both high ionic conductivity and oxidative stability (our approach). Reproduced with permission from Ref.^[32] Copyright (2020) American Chemical Society. f) Cycling performance of the cells with different electrolytes. Reproduced with permission from Ref.^[29] Copyright (2019) Wiley-VCH Verlag GmbH & Co. KGaA, Weinheim. g) The cycling stability of these three batteries. Reproduced with permission from Ref.^[34] Copyright (2015) WILEY-VCH Verlag GmbH & Co. KGaA, Weinheim. h) Current density of 0.2 mA cm⁻², area capacity limit protocol of 1.0 mAh cm⁻², using LHCE as electrolyte, voltage curve of cycle stability test. Reproduced with permission from Ref.^[35] Copyright (2020) American Chemical Society.

in reduced cycling stability. In view of the above mechanisms, the decomposition of ether electrolytes can be effectively inhibited by the following three strategies by (1) using a low polarity solvent to reduce the extraction of H from ether molecules by O₂⁻,^[29] (2) introducing additives to inhibit the production of free O₂⁻,^[30] (3) utilizing high concentration of Li salt to reduce the O₂⁻ lifetime.^[31]

Based on the above three strategies, the researchers have proposed the following specific improvement approaches. Firstly, modification is effective to improve the stability of ether electrolytes. The high ionic conductivity and oxidative stability of electrolytes can be achieved by covalently bonding the

fluorinated core with the ether “end group” as shown in Figure 3e.^[32] Among them, the fluorinated nucleus can deliver high oxidative stability, while the ether group provides high salt solubility and ionic conductivity. Huang et al.^[29] proposed a methylated cyclic ether, 2,2,4,4,5,5-hexamethyl-1,3-dioxolane (HMD) as a stable electrolyte solvent by molecular modification. The α -carbon of this ether molecule does not contain any hydrogen atoms so as to avoid the attack of O_2^- intermediates. Thus obtained LOBs can achieve 157 cycles, showing excellent stability (Figure 3f).

Secondly, additives can be introduced to accelerate the oxygen reduction/evolution reaction (ORR/OER) kinetics, thereby inhibiting the production of free O_2^- and improving the stability of ether-based electrolytes. Benzo-crown ethers (BCEs) are a type of electrolyte additives with different cavity sizes, which have strong binding affinity to Li^+ . During the charge process, these crown ether additives favor the decomposition of Li_2O_2 to form $Li_{2-x}O_2$ in the defect state through the strong binding force with Li^+ , thus accelerating OER. Meanwhile, the conjugated structure of benzene rings further enhances the cavity’s affinity to Li^+ through π orbitals, so BCE can also effectively promote ORR.^[33]

Finally, adjusting the electrolyte concentration is in favor of inhibiting the decomposition of ethers. Zhang et al.^[34] found that in a highly concentrated electrolyte, all DME molecules are coordinated with salt cations, and the C–H bond scission of DME becomes more difficult. In Figure 3g, LOBs with high-concentration electrolyte demonstrate greatly enhanced cycling stability under both full discharge/charge (2.0–4.5 V vs Li/Li⁺) and a cut-off capacity of 1000 mAh g⁻¹. However, the viscosity of electrolytes increases, and the conductivity and ability to dissolve oxygen decreases, so a locally high-concentration electrolyte has been further proposed. The high-concentration electrolyte (LHCE) was developed by using 1H,1H,5H-octafluoropentyl 1,1,2,2-tetrafluoroethyl ether (OTE) as the bleaching agent to decrease the viscosity and increase oxygen solubility.^[35] Besides improving the discharge capacity, the electrolyte had the ability to resist singlet oxygen attack. LHCE using OTE as an inert diluent has very good chemical and electrochemical properties in rechargeable LOBs (Figure 3h). Therefore, the use of a diluent does not affect the solvation structure under high-concentration electrolytes and meanwhile can enhance the electrochemical performance of LOBs.

2.4. Amide Electrolytes

Compared with carbonates and ethers, amide electrolytes have better stability against the O_2^- radical intermediate. Among them, dimethylformamide (DMF) has a high HOMO energy level, a strong negative ESP and a high DN.^[18] Additionally, it has also been reported as a solvent for reduced O_2 species.^[36]

Bruce et al.^[36b] found that although reactions at cathode are dominated by reversible Li_2O_2 formation/decomposition in the first charge/discharge cycle, electrolyte decomposition becomes anabolic during cycling as shown in Figure 4a. The byproduct of Li_2CO_3 cannot be completely decomposed after charge and

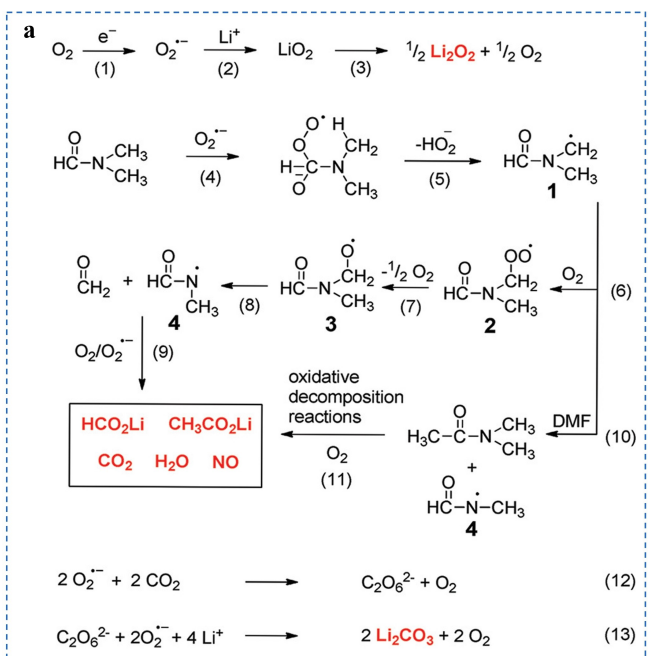


Figure 4. a) Proposed reaction mechanism during discharge. Reproduced with permission from Ref.^[36b] Copyright (2012) American Chemical Society. b) Dominant degradation mechanisms of carbonate-, ether-, and sulfoxide-based electrolytes and the molecular design of stable sulfamide- and sulfonamide-based solvents of BTMSA (top), DMCF₃SA (middle), and BMCF₃SA (bottom) for aprotic LOBs. Reproduced with permission from Ref.^[38] Copyright (2019) Elsevier Inc. c) Cyclic voltammetry on glass carbon working electrode performed at 50 mV s⁻¹ under argon atmosphere. Inset: Cyclic voltammogram for DMSO/LiClO₄ 0.100 M recorded in the potential range of DMSO stability (2.00 V to 4.50 V vs Li/Li⁺). Reproduced with permission from Ref.^[39] Copyright (2022) The Royal Society of Chemistry. d) Schematic illustrations of components in pure DMSO solvent, LiTFSI-12DMSO dilute electrolyte, LiTFSI-4DMSO concentrated electrolyte, and LiTFSI-3DMSO highly concentrated electrolyte. Reproduced with permission from Ref.^[40] Copyright (2017) WILEY-VCH Verlag GmbH & Co. KGaA, Weinheim.

will be continuously accumulated, resulting in capacity attenuation. Therefore, its stability to the oxygen reduction intermediates generated during the discharge process is still insufficient despite the stability of amide electrolytes is better than that of carbonate and ether electrolytes in terms of anti-oxidation stability. To remove the important substance that triggers side reactions— 1O_2 , Li et al.^[37] utilized electron-rich triphenylamine (TPA) as 1O_2 scavengers. This formed a complex intermediate of TPA and 1O_2 that altered the spin electronic direction through intersystem crossing, accelerating the conversion of 1O_2 to the ground state triplet oxygen (3O_2) and thereby inhibiting the side reactions induced by 1O_2 . LOBs containing TPA capture agents showed a reversibility of 2.04 e⁻/O₂ during charge, extending the cycle life to 310 cycles. The stability of the electrolyte can also be enhanced by rationally designing new molecular components. Three compounds—N-butyl-N,N,N'-trimethylsulfamide (BTMSA), N,N-dimethyl-trifluoromethanesulfonamide (DMCF₃SA), and N-butyl-N-methyl-tri-fluoromethanesulfonamide (BMCF₃SA) have been reported for use in aprotic LOBs (Figure 4b) and demonstrate exceptional stability under the diverse and harsh conditions present in LOBs cathode environment. For instance, these three compounds remain stable in the

presence of active substances such as peroxide, superoxide, and singlet O₂, while DMCF₃SA and BMCF₃SA are stable under electrochemical oxidation conditions (>4.5 V) due to the electron-absorbing CF₃ group, and the latter can be cycled 90 times in LOBs without capacity attenuation.^[38]

In addition, the lower LUMO level of amide-based electrolytes makes them highly reactive with Li anode.^[41] The LiTFSI/N,N-dimethyltrifluoro-acetamide (DMTFA) system supports the formation of the LiF-rich SEI on Li anode, showing low interface resistance and good cycling performance. Walker et al.^[42] demonstrated for the first time that Li anodes could be successfully cycled in the presence of N,N-dimethylacetamide (DMA) by using LiNO₃ to stabilize the SEI. Such a LOB can cycle for more than 2000 h at a current density of 0.1 mA cm⁻², and its stability should be attributed to the inertness of the amide core toward reactive oxygen species, combined with the ability of the nitrate anion to help form a protective inorganic SEI. Researchers also found that the battery could be stabilized by adjusting the solvation structure of Li⁺. Zhang et al.^[43] modulated the SEI film and free solvent molecules in medium electrolyte concentrations by modulating the Li⁺ solvation structure. The electrolyte, using DMA as solvent that contains 2 M LiTFSI and 1 M LiNO₃, promotes the formation of a LiF and LiN_xO_y coexisted inorganic-rich SEI film. As a result, Li anode can be protected from dendrite growth and corrosion, exhibiting enhanced kinetic and mass transfer processes. The cycle life of LOBs could be thus extended to 180 cycles. Similar to nitrile electrolytes, amide-based electrolytes can also form deep eutectic electrolyte (DEE) that better protect lithium metal.^[44] Solid N-methylacetamide (NMA) and LiTFSI are mixed in a 4:1 ratio. Since the large anion TFSI⁻ in LiTFSI is delocalized, both the cations and anions of LiTFSI interact with the polar groups of NMA to form DEE. The interfacial impedance of the lithium electrode in the DEE is low and grows slowly, enabling uniform lithium plating/stripping. The SEI contains more inorganic components such as Li_xN and LiF, exhibiting a smooth surface with no significant lithium dendrites, thereby overcoming the long-standing issue of incompatibility between lithium metal and amides. Furthermore, this NMA-based DEE possesses high ionic conductivity and excellent thermal, chemical, and electrochemical stability. Consequently, it demonstrates a high discharge capacity (8647 mAh g⁻¹), outstanding rate performance, and excellent cycling stability (280 cycles).

2.5. Sulfone Electrolytes

The extensively studied dimethyl sulfoxide (DMSO) is of high DN, strong ESP_{min}, and excellent salt solubility, which can form a strong conductive solution.^[11,18] Zhang et al.^[45] used 1.0 mol L⁻¹ LiTFSI/DMSO as electrolyte and porous graphene oxide as cathode to prepare LOBs that could deliver a discharge capacity of 10600 mAh g⁻¹, a charge overpotential of 3.7 V, and excellent rate performance. In another case, cyclic voltammogram (CV) in DMSO electrolytes identify the single-electron redox process of free-diffusing species by in situ electrochemical surface-enhanced Raman spectroscopy (SERS). It reveals that there is no

evidence of LiO₂ on cathode at any potential during discharge in DMSO electrolytes.^[10a] It is proved that DMSO can stably dissolve superoxide ions to promote the growth of discharge products according to the solution path and thereby increasing the discharge capacity. However, the low LUMO orbital energy of DMSO made it unstable towards Li metal, leading to Li dendrite growth and a series of side reactions. Furthermore, DMSO electrolytes also encounter decomposition issues during cycling the same as carbonate and ether electrolytes.

In order to improve the stability of DMSO towards Li anode, Zhao et al.^[46] proposed a method by using different polarity solvents (non-polar fluorosilane mixed with polar DMSO) to form a liquid-liquid interface to prevent DMSO from contacting anode. A thin inorganic SEI film is formed at anode to make Li⁺ uniformly deposited and inhibit the growth of Li dendrites. The cycling performance of LOBs containing this liquid-liquid interface could be thus improved by four times. When 1-methyl-3-benzyl-1H imidazolium bromide (IMPBr) was dissolved in DMSO, the IMP⁺ cations were preferentially diffused to the anode side and adsorbed on the surface of Li anode during charge.^[47] The electrostatic shielding effect of IMP⁺ inhibits the contact between DMSO, Br₃⁻ and Br₂ with Li anode and prevents side reactions. The formation of stable SEIs can effectively inhibit the side reaction, resulting in the relatively flat surface of anode.

In terms of the stability of the electrolyte itself, it is found that DMSO will react with O₂⁻ radicals, leading to the decomposition of the electrolyte. Silva et al.^[39] first investigated the influence of the imidazolium-based ionic liquid crystal (ILC) of 1-hexadecyl-3-methylimidazole bromide [C16mim][Br] as an additive for DMSO. ILC has the ability of self-aggregation, which enhances the stability of electrolyte. This aggregation reduces the number of free DMSO molecules for reaction during battery operation, thereby minimizing electrolyte degradation. The addition of ILC improves the stability of electrolyte, allowing 10 voltammetric cycles within an electrochemical window of 2.0 to 6.5 V relative to Li/Li⁺ as shown in Figure 4c.

It is reported that modulation of the solvation structure can simultaneously improve the stability of anode and electrolyte.^[40] For example, the LiTFSI-DMSO electrolyte could be employed to optimize the thickness of the corrosion layer on Li anode, showing high density of Li metal and block retention rates. After 90 cycles, the surface of carbon nanotube electrode could well remain its network structure. According to literature reports, Li⁺ normally prefers to form four coordination bonds with solvent molecules and/or salt anions as illustrated in Figure 4d,^[48] and the highly concentrated LiTFSI-DMSO electrolyte should contain only TFSI⁻-Li⁺-(DMSO)₃ complexes, leaving no free DMSO molecules. Such a salt-solvent complex is of a higher Gibbs activation energy barrier than that of the free DMSO solvent molecules, which has good resistance to the attack of superoxide radical anions to reduce the decomposition of electrolytes.

2.6. Multi-Component Electrolytes

The traditional electrolyte only consists of a solvent, a salt, and an additive, which is hard to simultaneously meet the advanced requirements of the electrochemical window, the solvent structure, and the growth kinetics of discharge products. Based on this, researchers have been focused on the development of multi-component electrolytes. In general, solvents can be classified according to DN that is a quantitative description of Lewis base to express the solvent's ability to dissolve cations and Lewis acids. According to the Hard-Soft-Acid-Base theory, Li^+ is a hard Lewis acid with high affinity to hard Lewis bases, such as high DN solvents.^[36a] The coordination bond strength between Li^+ and solvent directly determines the acidity of Li^+ , thereby allowing for adjustment of the solvation structure. In high DN solvents, due to the stronger bond of $\text{Li}^+-(\text{solvent})_n$, the acidity of Li^+ decreases more than that in low DN solvents, so the high DN number solvent can better dissolve Li salt to form SSE.^[49] At this point, O_2^- as a moderate soft base can remain stable for longer periods in high DN solvents, facilitating the formation of soluble Li_2O_2 and resulting in the generation of ring-shaped Li_2O_2 particles. However, the SEI derived from SSE is consistently rich in organic components, exhibiting lower Li^+ conductivity and mechanical strength, and thereby fails to suppress the growth of Li dendrites. On the contrary, WSE is formed in low DN solvents, showing significantly lower dissolution capability.^[50] Consequently, anions will participate more in the solvation sheath structure of Li^+ , which is apt to form inorganic-rich SEIs that could enhance mechanical strength, accelerate Li^+ transfer, and induce uniform Li deposition. However, WSE demonstrated a limited stabilization time for O_2^- , causing the discharge products to grow along a surface-adsorption pathway into the film-like Li_2O_2 (Figure 5a). This film blocks the cathode surface, leading to rapid battery degradation.

Cao et al.^[51] proposed an electron donor modulation strategy by using high DN solvent (DMSO) with strong electron donor capability to dissolve Li salts, while low DN solvent (PC) with weak electron donor capability to coordinate sparingly with Li^+ and primarily act as diluent to disperse large AGG clusters into CIP structures (Figure 5b). It results in the formation of CIP structures in the $\text{LiNO}_3\text{-DMSO@PC}$ electrolyte. The LUMO energy level of the CIP structure is higher than that of AGG, resulting in an expanded electrochemical window. Thereby, the electrolyte exhibits excellent reduction stability and long cycling performance. Similarly the combination of DMSO (high DN) and TEGDME (low DN) leads to the formation of locally strong solvation effect electrolyte (LSSE) as illustrated in Figure 5c.^[52] In this configuration, DMSO and TFSI^- bind with Li^+ to form robust solvating clusters as the first coordination shell, while TEGDME molecules distribute around them as the second shell. Such a LSSE provides a high capacity of approximately $3528 \text{ mAh g}_{\text{carbon}}^{-1}$ with good cycling performance by combining the solubility of high DN solvents with the stability of low DN ones (Figure 5d). It is found that a stable SEI could be formed with few byproducts derived from electrolyte decomposition. In addition, LOBs with 4 M LiNO_3 dissolved in N-

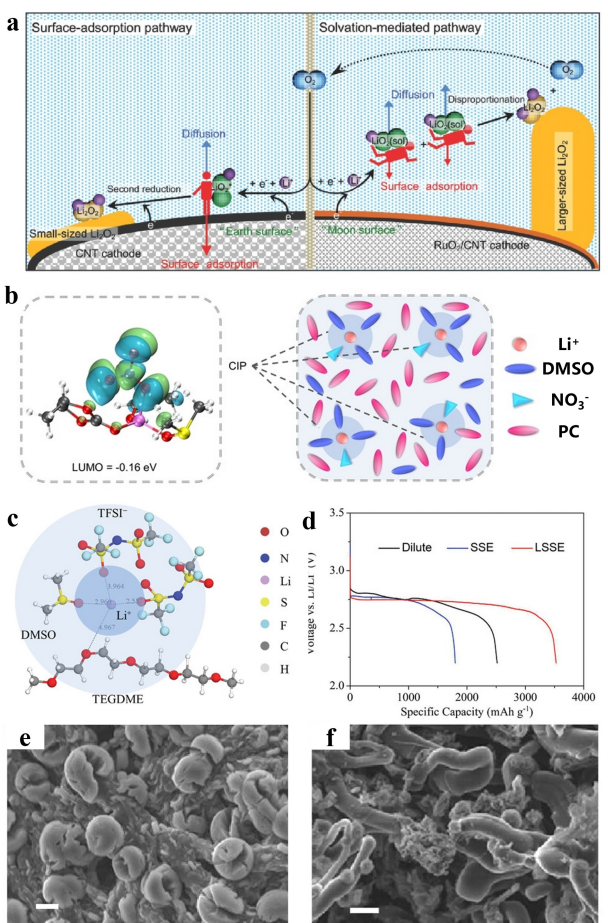


Figure 5. a) Schematic of the Li_2O_2 growth mechanism. Reproduced with permission from Ref.^[8] Copyright (2016) WILEY-VCH Verlag GmbH & Co. KGaA, Weinheim. b) The schematic diagrams of $\text{LiNO}_3\text{-DMSO@PC}$ electrolyte with CIPs. Reproduced with permission from Ref.^[51] Copyright (2024) Wiley-VCH GmbH. c) MD simulations of the molecular structures of LSSE. Reproduced with permission from Ref.^[52] Copyright (2021) Wiley-VCH GmbH. d) The full discharge performance of the LOBs with the KB cathodes at a current density. Reproduced with permission from Ref.^[52] Copyright (2021) Wiley-VCH GmbH. e) SEM image of carbon electrode after discharge. Scale bars are 1 μm . Reproduced with permission from Ref.^[53] Copyright (2023) American Chemical Society. f) SEM image of Li electrode after 10th cycle. Scale bars are 1 μm . Reproduced with permission from Ref.^[53] Copyright (2023) American Chemical Society.

methylpyrrolidone (NMP)/50 vol % bis (2,2,2-trifluoroethyl) ether (BTFE) exhibited a stable discharge/charge behavior at a high current density of 1.0 mAcm^{-2} and a high area capacity of 2.0 mAhcm^{-2} .^[53] The result shows that the multi-component electrolyte accelerates the solution path to form large sized Li_2O_2 toroids (Figure 5e). BTFE decomposes to form the LiF-rich SEI, which improves the reversibility of Li deposition/dissolution (Figure 5f). Solvation entropy is also an important evaluation metric for the solvation structure of electrolytes. Wang et al.^[54] proposed an innovative entropy-driven solubilization strategy for LiNO_3 . Adding multivalent ester GTA(glyceryl triacetate) to the EC and dimethyl carbonate (DMC) electrolyte effectively reduces the entropy penalty of the coordination process. The multiple ester group binding sites of GTA facilitate the dissolution of LiNO_3 , forming an anion-rich solvation structure

and reducing the number of free solvent molecules. Consequently, the EC-GTA-DMC electrolyte features a rich inorganic SEI and an improved electrochemical window, resulting in a high Coulombic efficiency of 99% and enhanced cycling stability.”

3. Additives in Electrolyte

Additives in electrolyte can significantly influence the reaction mechanism, and thus the discharge capacity and reversibility. This section will focus on the critical and unique additive, redox mediators (RMs). They are commonly used additives that effectively address the issue of high charge overpotential caused by slow LOB kinetics, thereby preventing electrolyte decomposition. During the discharge process, the accumulation of Li_2O_2 at cathode will lead to the increase of overpotential required for its decomposition. While for charge, the elevated overpotential subsequently induces severe side reactions.^[55] The incorporation of RMs into electrolyte can mitigate these challenges. During charge, RM is first oxidized to RM^+ at cathode, which is then converted to RM by catalyzing the chemical decomposition of Li_2O_2 . For example, during discharge, 1-methyl-3-benzyl-1H imidazolium bromide (IMPBr) could form IMP^+ , which exhibits strong binding affinity to the intermediate product O_2^- , while Br^- strongly binds to Li^+ , promoting the solvation process.^[47] During charge, Br^- mediates the decomposition of the discharge products, thereby reducing the charge overpotential and accelerating the reaction rate.

Although RMs are effective to reduce the overpotential of LOBs, the diffusion of RMs can lead to Li anode corrosion, thereby decreasing the round-trip efficiency of the battery.^[56] It has been demonstrated that Br-containing RMs can generate an inorganic SEI film on anode, effectively inhibiting the shuttle effect. For example, BrCH_2NO_2 could serve as a bifunctional RM to be chemically reduced on Li anode to form bromide ions (Br^-), which in situ create a protective layer to inhibit the shuttle effect. Furthermore, this protective layer facilitates effective Li^+ transfer, resulting in uniform Li deposition without dendrite formation, and contributes to an extended cycle life of the LOBs (more than 120 cycles, Figure 6a).^[57] In another case of MgBr_2 , it has been utilized as both a RM and a SEI film-forming agent.^[58] As a result, Br_3^- generated from MgBr_2 facilitate the decomposition of Li_2O_2 , thereby reducing the battery's overpotential. Simultaneously, the spontaneous reaction between Mg^{2+} and Li anode in the O_2 environment induces the formation of a uniform SEI film composed of Mg and MgO (Figure 6b). Li et al.^[59] synthesized a polymer-based composite protective separator incorporating molecular sieves to mitigate the shuttle effect associated with 2,2,6,6-tetramethylpiperidinyloxy (TEMPO). The pores in zeolite with a diameter of 4 Å are capable of physically blocking the migration of larger TEMPO molecules. By aid of zeolite molecular sieves, the cycle life of LOBs can be significantly extended from 20 to 170 cycles at a current density of 250 mA g^{-1} at a limited capacity of 500 mAh g^{-1} .

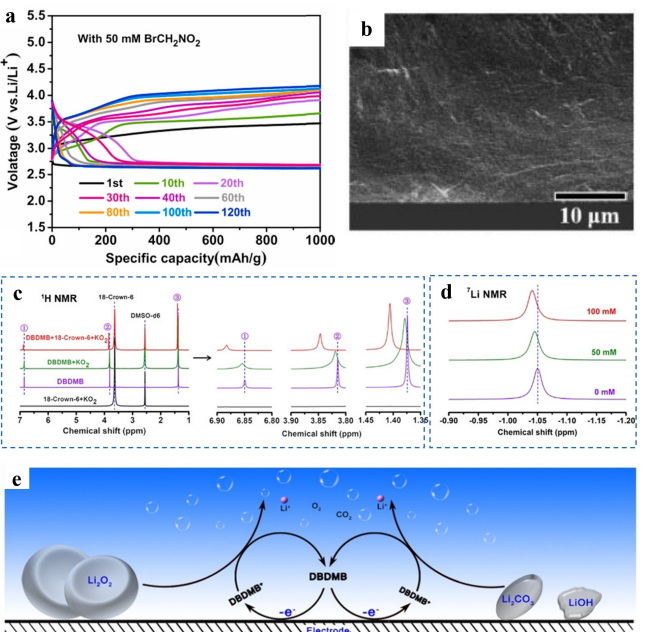


Figure 6. a) Cycling performance of the battery with BrCH_2NO_2 additive at 500 mA g^{-1} . Reproduced with permission from Ref.^[57] Copyright (2021) Elsevier B.V. b) SEM images of Li anodes in a LOBs with MgBr_2 electrolytes after cycles. Reproduced with permission from Ref.^[58] Copyright (2024) Elsevier B.V. c) ^1H NMR spectra of DBDMB with/without O_2^- . Reproduced with permission from Ref.^[60] Copyright (2020) Wiley-VCH GmbH. d) ^{7}Li NMR spectra of electrolytes with different concentrations of DBDMB. Reproduced with permission from Ref.^[60] Copyright (2020) Wiley-VCH GmbH. e) Schematic illustration of the oxidation reaction mechanism of DBDMB towards Li_2O_2 , LiOH and Li_2CO_3 in LOBs. Reproduced with permission from Ref.^[60]. Copyright (2020) Wiley-VCH GmbH.

Different from the most reported bifunctional additives, Zhang et al.^[60] introduced a novel trifunctional ether RM, 2,5-di-tert-butyl-1,4-dimethoxybenzene (DBDMB), which not only encompassed the functionalities of the aforementioned RMs but also captured the intermediate of O_2^- (Figure 6c). Moreover, the formation of solvated structures between DBDMB and Li^+ (Figure 6d) accelerated the ORR kinetics and the growth of Li_2O_2 via the solution pathway. Figure 6e depicts the charge/discharge cycle of RMs, illustrating its ability to simultaneously facilitate the charge process by co-decomposing Li_2O_2 , Li_2CO_3 and LiOH and to improve the discharge process by capturing O_2^- . Furthermore, the adsorption energy of O_2 by DBDMB is significantly higher than the reported value of -0.82 eV for O_2 absorption at the carbon cathode, which helps prevent O_2^- from inducing carbon degradation.^[8,61] Such obtained LOB exhibited a high Li_2O_2 generation efficiency of 96.60% and a very low residual rate of 0.97% after the subsequent recharge process.

4. Conclusion and Outlook

For years, great efforts have been devoted to developing the non-aqueous liquid electrolytes of LOBs, however, it is still unsatisfactory for practical applications. In the electrolyte, the solvent serves to dissolve the electrolyte salt and provides a

medium for Li^+ migration. Lithium salts contribute ionic conductivity and participates in the solvation structure with solvent molecules. While, the introduction of RMs into the electrolyte can effectively mitigate the issue of high charge overpotential caused by slow LOBs kinetics. Therefore, an ideal electrolyte should firstly possess good chemical/electrochemical stability during battery operation. Secondly, it should form a solvent-solvating structure that competes with anions and solvent molecules, thereby forming inorganic-rich SEIs to enhance battery reversibility and coulombic efficiency. Thirdly, it should facilitate the generation of Li_2O_2 through the solution pathway to promote the battery capacity.

As previously mentioned, most current works have been focusing on the single-salt, single-solvent systems, which are insufficient to meet the practical requirements of LOBs. Consequently, an alternative approach is to mix solvents and salts with different functionalities to design multi-component electrolytes. This strategy leverages competitive solvation structures to exploit the advantages of each component. However, the interaction mechanisms among the components in multi-component electrolytes are highly complex. The modulation index between components is quite sensitive, making adjustments difficult, and it often requires an extended research period. Recently, machine learning methods have shown great potential in significantly reducing time costs and improving research and development efficiency. In the future, by integrating experimental approaches with predictive machine learning methods, it may be possible to discover advanced electrolytes that are perfectly suited for LOBs, enabling their stable operation.

Acknowledgements

This work was financially supported by the National Natural Science Foundation of China (Grant no. 51925202, U23A20575, and U22A20141).

Conflict of Interests

The authors declare no conflict of interest.

Keywords: LOBs • Non-aqueous liquid electrolytes • Design of electrolyte

- [1] A. Kondori, M. Esmaeilirad, A. M. Harzandi, R. Amine, M. T. Saray, L. Yu, T. Liu, J. Wen, N. Shan, H.-H. Wang, A. T. Ngo, P. C. Redfern, C. S. Johnson, K. Amine, R. Shahbazian-Yassar, L. A. Curtiss, M. Asadi, *Science* **2023**, 379, 499.
- [2] K. M. Abraham, Z. Jiang, *J. Electrochem. Soc.* **1996**, 143, 1.
- [3] H. Yu, D. Liu, X. Feng, Y. Zhang, *Nano Select* **2020**, 1, 79.
- [4] a) B. D. McCloskey, D. S. Bethune, R. M. Shelby, G. Girishkumar, A. C. Luntz, *J. Phys. Chem. Lett.* **2011**, 2, 1161; b) G. Girishkumar, B. McCloskey, A. C. Luntz, S. Swanson, W. Wilcke, *J. Phys. Chem. Lett.* **2010**, 1, 2193.
- [5] a) J.-S. Lee, S. Tai Kim, R. Cao, N.-S. Choi, M. Liu, K. T. Lee, J. Cho, *Adv. Energy Mater.* **2011**, 1, 34; b) P. He, T. Zhang, J. Jiang, H. Zhou, *J. Phys. Chem. Lett.* **2016**, 7, 1267.
- [6] Y. Liao, M. Zhou, L. Yuan, K. Huang, D. Wang, Y. Han, J. Meng, Y. Zhang, Z. Li, Y. Huang, *Adv. Energy Mater.* **2023**, 13, 2301477.
- [7] Z. Piao, R. Gao, Y. Liu, G. Zhou, H. M. Cheng, *Adv. Mater.* **2023**, 35, 2206009.
- [8] J. J. Xu, Z. W. Chang, Y. Wang, D. P. Liu, Y. Zhang, X. B. Zhang, *Adv. Mater.* **2016**, 28, 9620.
- [9] P. Zhang, M. Ding, X. Li, C. Li, Z. Li, L. Yin, *Adv. Energy Mater.* **2020**, 10, 2001789.
- [10] a) L. Johnson, C. Li, Z. Liu, Y. Chen, S. A. Freunberger, P. C. Ashok, B. B. Praveen, K. Dholakia, J.-M. Tarascon, P. G. Bruce, *Nat. Chem.* **2014**, 6, 1091; b) G. Leverick, Y. Shao-Horn, *Adv. Energy Mater.* **2023**, 13, 2204094; c) F. Karcher, M. Uhl, T. Geng, T. Jacob, R. Schuster, *Angew. Chem. Int. Ed.* **2023**, 62, e202301253.
- [11] K. Chen, X. Shen, L. Luo, H. Chen, R. Cao, X. Feng, W. Chen, Y. Fang, Y. Cao, *Angew. Chem. Int. Ed.* **2023**, 62, e202312373.
- [12] T. Ogasawara, A. Debart, M. Holzapfel, P. Novak, P. G. Bruce, *J. Am. Chem. Soc.* **2006**, 128, 1390.
- [13] W. Zhang, T. Yang, X. Liao, Y. Song, Y. Zhao, *Energy Storage Mater.* **2023**, 57, 249.
- [14] W. Xu, V. V. Viswanathan, D. Wang, S. A. Towne, J. Xiao, Z. Nie, D. Hu, J.-G. Zhang, *J. Power Sources* **2011**, 196, 3894.
- [15] J. W. Mullinax, C. W. Bauschlicher, J. W. Lawson Jr., *J. Phys. Chem. A* **2021**, 125, 2876.
- [16] A. T. S. Freiberg, M. K. Roos, J. Wandt, R. de Vivie-Riedle, H. A. Gasteiger, *J. Phys. Chem. A* **2018**, 122, 8828.
- [17] S. A. Freunberger, Y. Chen, Z. Peng, J. M. Griffin, L. J. Hardwick, F. Barde, P. Novak, P. G. Bruce, *J. Am. Chem. Soc.* **2011**, 133, 8040.
- [18] Y. Wu, Q. Hu, H. Liang, A. Wang, H. Xu, L. Wang, X. He, *Adv. Energy Mater.* **2023**, 13, 2300259.
- [19] Z. Peng, S. A. Freunberger, L. J. Hardwick, Y. Chen, V. Giordani, F. Barde, P. Novak, D. Graham, J. M. Tarascon, P. G. Bruce, *Angew. Chem. Int. Ed.* **2011**, 50, 6351.
- [20] R. Younesi, P. Norby, T. Vegge, *ECS Electrochem. Lett.* **2014**, 3, A15.
- [21] Z. Peng, X. Cao, P. Gao, H. Jia, X. Ren, S. Roy, Z. Li, Y. Zhu, W. Xie, D. Liu, Q. Li, D. Wang, W. Xu, J. G. Zhang, *Adv. Funct. Mater.* **2020**, 30, 2001285.
- [22] V. S. Bryantsev, J. Uddin, V. Giordani, W. Walker, G. V. Chase, D. Addison, *J. Am. Chem. Soc.* **2014**, 136, 3087.
- [23] N. D. Trinh, D. Lepage, D. Aymé-Perron, A. Badia, M. Dollé, D. Rochefort, *Angew. Chem. Int. Ed.* **2018**, 57, 5072.
- [24] Z. Hu, F. Xian, Z. Guo, C. Lu, X. Du, X. Cheng, S. Zhang, S. Dong, G. Cui, L. Chen, *Chem. Mater.* **2020**, 32, 3405.
- [25] V. S. Bryantsev, V. Giordani, W. Walker, M. Blanco, S. Zecevic, K. Sasaki, J. Uddin, D. Addison, G. V. Chase, *J. Phys. Chem. A* **2011**, 115, 12399.
- [26] B. D. McCloskey, A. Valery, A. C. Luntz, S. R. Gowda, G. M. Wallraff, J. M. Garcia, T. Mori, L. E. Krupp, *J. Phys. Chem. Lett.* **2013**, 4, 2989.
- [27] D. Zhu, L. Zhang, M. Song, X. Wang, J. Mei, L. W. M. Lau, Y. Chen, *J. Solid State Electrochem.* **2013**, 17, 2865.
- [28] X. Liu, X. Song, Q. Zhang, X. Zhu, Q. Han, Z. Liu, P. Zhang, Y. Zhao, *J. Energy Chem.* **2022**, 69, 516.
- [29] Z. Huang, H. Zeng, M. Xie, X. Lin, Z. Huang, Y. Shen, Y. Huang, *Angew. Chem. Int. Ed.* **2019**, 58, 2345.
- [30] X. Gao, Y. Chen, L. Johnson, P. G. Bruce, *Nat. Mater.* **2016**, 15, 882.
- [31] a) C. Hwang, J. Yoo, G. Y. Jung, S. H. Joo, J. Kim, A. Cha, J. G. Han, N. S. Choi, S. J. Kang, S. Y. Lee, S. K. Kwak, H. K. Song, *ACS Nano* **2019**, 13, 9190; b) J. Scheers, D. Lidberg, K. Sodeyama, Z. Futera, Y. Tateyama, *Phys. Chem. Chem. Phys.* **2016**, 18, 9961.
- [32] C. V. Amanchukwu, Z. Yu, X. Kong, J. Qin, Y. Cui, Z. Bao, *J. Am. Chem. Soc.* **2020**, 142, 7393.
- [33] Q. Zhang, Y. Li, E. T. Poh, Z. Xing, M. Zhang, M. Wang, Z. Sun, J. Pan, S. V. C. Vummala, J. Zhang, W. Chen, *Adv. Energy Mater.* **2023**, 13, 2301748.
- [34] B. Liu, W. Xu, P. Yan, X. Sun, M. E. Bowden, J. Read, J. Qian, D. Mei, C. M. Wang, J. G. Zhang, *Adv. Funct. Mater.* **2015**, 26, 605.
- [35] W.-J. Kwak, S. Chae, R. Feng, P. Gao, J. Read, M. H. Engelhard, L. Zhong, W. Xu, J.-G. Zhang, *ACS Energy Lett.* **2020**, 5, 2182.
- [36] a) V. S. Bryantsev, J. Uddin, V. Giordani, W. Walker, D. Addison, G. V. Chase, *J. Electrochem. Soc.* **2012**, 160, A160; b) Y. Chen, S. A. Freunberger, Z. Peng, F. Barde, P. G. Bruce, *J. Am. Chem. Soc.* **2012**, 134, 7952.
- [37] Z. Jiang, Y. Huang, Z. Zhu, S. Gao, Q. Lv, F. Li, *Proc. Natl. Acad. Sci. U. S. A* **2022**, 119, e2202835119.
- [38] S. Feng, M. Huang, J. R. Lamb, W. Zhang, R. Tatara, Y. Zhang, Y. G. Zhu, C. F. Perkins, J. A. Johnson, Y. Shao-Horn, *Chem* **2019**, 5, 2630.
- [39] T. C. Lourenço, L. M. S. Barros, C. G. Ancheta, T. C. M. Nepel, J. P. O. Júlio, L. G. Dias, R. M. Filho, G. Doubek, J. L. F. Da Silva, *J. Mater. Chem. A* **2022**, 10, 11684.

- [40] B. Liu, W. Xu, P. Yan, S. T. Kim, M. H. Engelhard, X. Sun, D. Mei, J. Cho, C. M. Wang, J. G. Zhang, *Adv. Energy Mater.* **2017**, *7*, 1602605.
- [41] V. S. Bryantsev, V. Giordani, W. Walker, J. Uddin, I. Lee, A. C. T. van Duin, G. V. Chase, D. Addison, *J. Phys. Chem. C* **2013**, *117*, 11977.
- [42] W. Walker, V. Giordani, J. Uddin, V. S. Bryantsev, G. V. Chase, D. Addison, *J. Am. Chem. Soc.* **2013**, *135*, 2076.
- [43] Y. Yu, G. Huang, J.-Y. Du, J.-Z. Wang, Y. Wang, Z.-J. Wu, X.-B. Zhang, *Energy Environ. Sci.* **2020**, *13*, 3075.
- [44] C. L. Li, G. Huang, Y. Yu, Q. Xiong, J. M. Yan, X. B. Zhang, *J. Am. Chem. Soc.* **2022**, *144*, 5827.
- [45] D. Xu, Z.-L. Wang, J.-J. Xu, L.-L. Zhang, X.-B. Zhang, *Chem. Commun.* **2012**, *48*, 6948.
- [46] X. He, X. Liu, Q. Han, P. Zhang, X. Song, Y. Zhao, *Angew. Chem. Int. Ed.* **2020**, *59*, 6397.
- [47] J. Lai, N. Chen, F. Zhang, B. Li, Y. Shang, L. Zhao, L. Li, F. Wu, R. Chen, *Energy Storage Mater.* **2022**, *49*, 401.
- [48] a) S. Yanase, T. Oi, *J. Nucl. Sci. Technol.* **2002**, *39*, 1060; b) E. Cazzanelli, F. Croce, G. B. Appetecchi, F. Benevelli, P. Mustarelli, *J. Chem. Phys.* **1997**, *107*, 5740; c) R. J. Blint, *J. Electrochem. Soc.* **1995**, *142*, 696.
- [49] X. Zhang, L. Zou, Y. Xu, X. Cao, M. H. Engelhard, B. E. Matthews, L. Zhong, H. Wu, H. Jia, X. Ren, P. Gao, Z. Chen, Y. Qin, C. Kompella, B. W. Arey, J. Li, D. Wang, C. Wang, J. G. Zhang, W. Xu, *Adv. Energy Mater.* **2020**, *10*, 2000368.
- [50] R. Xu, J. F. Ding, X. X. Ma, C. Yan, Y. X. Yao, J. Q. Huang, *Adv. Mater.* **2021**, *33*, e2105962.
- [51] H. Chen, K. Chen, L. Luo, X. Liu, Z. Wang, A. Zhao, H. Li, X. Ai, Y. Fang, Y. Cao, *Angew. Chem. Int. Ed.* **2024**, e202316966.
- [52] J. Lai, H. Liu, Y. Xing, L. Zhao, Y. Shang, Y. Huang, N. Chen, L. Li, F. Wu, R. Chen, *Adv. Funct. Mater.* **2021**, *31*, 2101831.
- [53] M. Ono, S. Matsuda, *ACS Appl. Energ. Mater.* **2023**, *6*, 3357.
- [54] Z. Jin, Y. Liu, H. Xu, T. Chen, C. Wang, *Angew. Chem. Int. Ed.* **2024**, *63*, e202318197.
- [55] J. Christensen, P. Albertus, R. S. Sanchez-Carrera, T. Lohmann, B. Kozinsky, R. Liedtke, J. Ahmed, A. Kojic, *J. Electrochem. Soc.* **2011**, *159*, R1.
- [56] a) Y. Chen, S. A. Freunberger, Z. Peng, O. Fontaine, P. G. Bruce, *Nat. Chem.* **2013**, *5*, 489; b) W.-J. Kwak, S.-J. Park, H.-G. Jung, Y.-K. Sun, *Adv. Energy Mater.* **2018**, *8*, 1702258.
- [57] X.-P. Zhang, Y.-N. Li, J.-W. Deng, Y. Mao, J.-Y. Xie, T. Zhang, *J. Power Sources* **2021**, *506*, 230181.
- [58] G. Sun, Y. Wang, D. Yang, Z. Zhang, W. Lu, M. Feng, *Chin. Chem. Lett.* **2024**, *35*, 108469.
- [59] X. Wu, H. Wu, S. Guan, Y. Liang, K. Wen, H. Wang, X. Wang, C.-W. Nan, L. Li, *Nano Res.* **2023**, *16*, 9453.
- [60] Q. Xiong, G. Huang, X. B. Zhang, *Angew. Chem. Int. Ed.* **2020**, *59*, 19311.
- [61] Y. Zhang, L. Wang, X. Zhang, L. Guo, Y. Wang, Z. Peng, *Adv. Mater.* **2018**, *30*, 1705571.

Manuscript received: August 16, 2024

Revised manuscript received: October 8, 2024

Accepted manuscript online: October 12, 2024

Version of record online: November 13, 2024